

# Plane shockwave generation in liquid water using irradiation of terahertz pulses

Masaaki Tsubouchi,<sup>1,\*</sup> Hiromichi Hoshina,<sup>2</sup> Masaya Nagai,<sup>3</sup> and Goro Isoyama<sup>4</sup>

<sup>1</sup>Kansai Photon Science Institute, National Institutes for Quantum and Radiological Science and Technology (QST), 8-1-7 Umimedai, Kizugawa, Kyoto 619-0215, Japan

<sup>2</sup>RIKEN Center for Advanced Photonics, RIKEN, 519-1399 Aramaki-Aoba, Aoba-ku, Sendai, 980-0845, Japan

<sup>3</sup>Graduate School of Engineering Science, Osaka University, 1-3 Machikaneyama, Toyonaka, Osaka 560-8531, Japan

<sup>4</sup>Institute of Scientific and Industrial Research (ISIR), Osaka University, 8-1 Mihogaoka, Ibaraki, Osaka, 567-0047, Japan

\*Author to whom correspondence should be addressed: [tsubouchi.masaaki@qst.go.jp](mailto:tsubouchi.masaaki@qst.go.jp)

## ABSTRACT

We demonstrate shockwave propagation with a plane wave front in liquid water using a terahertz (THz) laser pulse. The THz light can effectively generate the shockwave in water due to strong absorption via a stretching vibration mode of the hydrogen bonding network. This produces a plane shockwave from a large area excitation of the water surface irradiated by loosely focused THz light. This contrasts with conventional spherical shockwaves triggered by plasma generation via multi-photon absorption of near-infrared light. The shockwave generation and the plane wave propagation were observed using a system with a THz free electron laser and shadowgraph imaging. The plane shockwave was generated by small irradiation energy density of THz light,  $0.3 \text{ GW/cm}^2$ , and delivered 100 times deeper than the penetration depth for water. The THz-light-induced plane shockwave offers great advantages compared to the spherical shockwave, and it will open non-thermal operations for industrial and biological applications.

Laser-induced breakdown (LIB) is one of the phenomena induced by intense laser light in a transparent medium.<sup>1,2</sup> LIB is followed by thermal, acoustic, and mechanical effects on matter that trigger and control specific chemical and biological reactions in unconventional ways. Especially in liquid such as aqueous solutions, LIB is attractive as an innovative method for use in medical applications.<sup>3,4</sup>

LIB is a destructive process based on dielectric breakdown and subsequent plasma generation, resulting in serious risks of damage to the materials and biological tissues. To avoid unwanted damage to the sample, the LIB process is caused on an air–water interface apart from the sample followed by shockwave generation and propagation through water.<sup>5</sup> The shockwave delivers the laser photon energy as the mechanical one to the sample in water. The laser induced shockwave has been demonstrated with high-power CO<sub>2</sub> laser light with a wavelength of 10.6  $\mu\text{m}$  and a sub-microsecond pulse,<sup>6-8</sup> a femtosecond X-ray laser pulse<sup>9,10</sup> and so on, and it has been applied in machining, surgery, and drug delivery.

In previous laser-induced shockwave studies, the near- or mid-IR laser light is tightly focused at a specific point, and then, the spherical shockwave is generated from the point source as shown in Fig. 1(a). The intensity of the spherical wave rapidly drops during propagation; therefore, the target should be close to the source of the shockwave. On the other hand, the plane-like shockwave is superior to the spherical one for practical use because the plane wave can be delivered without intensity drop over long distances (Fig. 1(b)), and geometrical control such as reflection and focusing onto the target can be easily carried out.

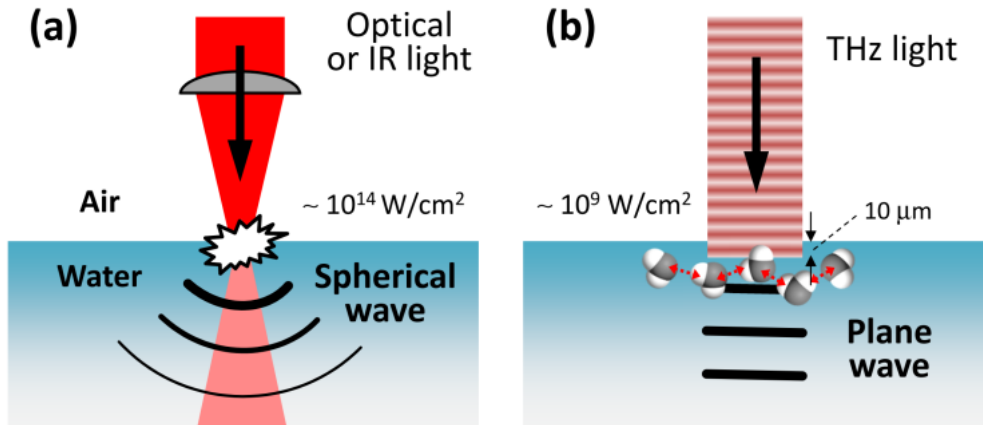


Fig. 1. Mechanisms of shockwave generation in the air–water interface. (a) Optical or IR laser generates the spherical-like shockwave from the point source by the intense laser field with tight focusing. (b) THz laser, by contrast, can generate the plane-like shockwave by the relatively weak field with loose focusing.

To realize the plane wave propagation in water, we propose a terahertz (THz)-light-induced shockwave. Because a large-area source is required for the plane shockwave propagation based on Huygens' principle, efficient energy conversion from the light source to the shockwave is necessary. We then adopt a THz laser pulse as the irradiation light source for shockwave generation. The THz light has a frequency of  $10^{12}$  Hz, which lies between the frequency ranges of light and radio waves. Due to resonance of the intermolecular vibration in the hydrogen-bonding network of liquid water around 5 THz,<sup>11,12</sup> the THz light is completely absorbed very close to the surface of the water with a penetration depth of  $10 \mu\text{m}$ . The strong absorption induces a rapid and local pressure increase followed by the plane shockwave generation effectively. In addition, the low photon energy (4 meV at 1 THz) of the THz light does not induce any ionization, dissociation, or structural changes in the molecules. This is a great advantage of THz light for non-destructive shockwave generation in industrial and medical applications.

In this study, we demonstrate shockwave generation with THz light provided by a free electron laser (FEL) and detect it using the shadowgraph method with 10 ns time and  $15 \mu\text{m}$  spatial resolutions. The characteristics of the THz shockwave are investigated by observing the spatiotemporal evolution. We conclude this study with perspectives on the THz-light-induced shockwave.

For the THz light source to generate the shockwave, we employed the THz-FEL on the L-band electron linear accelerator (LINAC) at the Research Laboratory for Quantum Beam Science, Institute of Science and Industrial Research, Osaka University.<sup>13-16</sup> The detailed characteristics and the evaluation method of THz pulses from the FEL were described in the previous paper.<sup>14</sup> Linearly polarized THz macropulses are generated by the THz-FEL at a repetition rate of 5 Hz with the highest pulse energy of 50 mJ. Fig. 2(a) shows a THz macropulse structure measured with a fast pyroelectric detector. The macropulse contains a train of about 150 micropulses separated at 36.9 ns intervals (27 MHz repetition). The highest micropulse energy was estimated to be 350  $\mu$ J, which is far and away the largest THz-FEL micropulse energy in the world. The temporal width of the micropulse was measured to be 1.7 ps by an electro-optic sampling technique.<sup>17, 18</sup> The center frequency was 4 THz, which corresponds to a lower frequency edge of the absorption band due to the intermolecular vibration in liquid water. At this frequency, the absorption coefficient of liquid water is 800  $\text{cm}^{-1}$ ,<sup>11</sup> which implies that more than 99.7% of irradiated energy is absorbed within 0.1 mm of the surface.

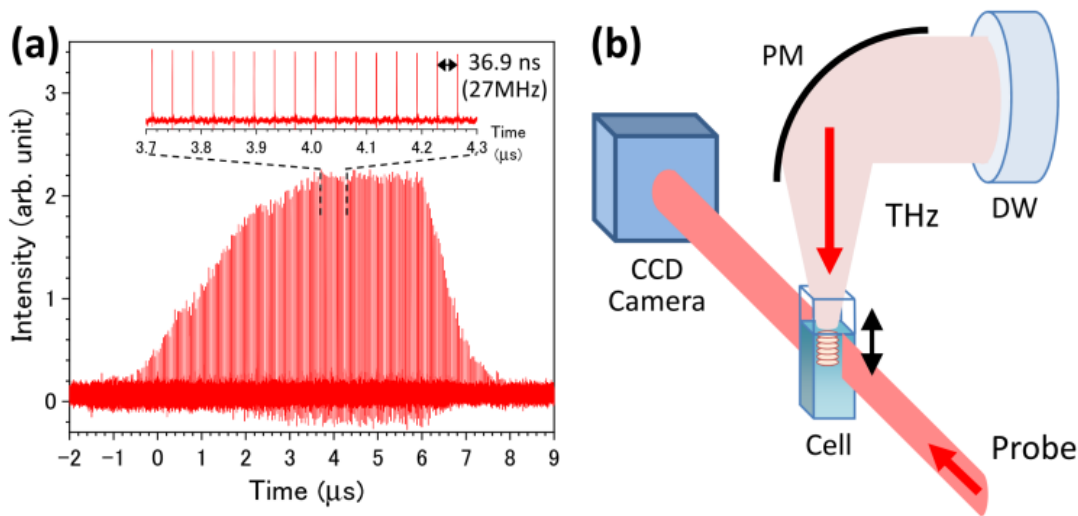


Fig. 2. (a) Macropulse structure containing a train of approximately 150 micropulses. Inset shows the enlarged micropulse train with the interval of 36.9 ns (a repetition rate of 27 MHz). (b) Experimental setup for generating and probing the THz-FEL-induced shockwave on an air–water interface. DW: polycrystalline diamond window, PM: off-axis gold-coated parabolic mirror with a focal length of 50 mm, cell: quartz sample cell on a lab jack to adjust a focus diameter of the THz light on the air–water interface.

Fig. 2(b) shows a schematic diagram of the shockwave generation and observation system. The THz light passing through a polycrystalline diamond window from the evacuated FEL system into the air was loosely focused on the distilled water sample using a gold-coated off-axis parabolic mirror with a 50 mm focal length. To evaluate a spot size of the THz pulse on the water surface, we used a knife-edge method and estimated it to be 0.7 mm at full width at half maximum. The input pulse energy was attenuated with the THz attenuators (TYDEX), which contained wedged silicon wafers with different attenuation levels.

A two-dimensional cross-section image of the shockwave was observed using a shadowgraph technique, which clearly shows an inhomogeneous density distribution in transparent media.<sup>19</sup> In the shadowgraph image, the signal intensity depends on the second derivative of the refractive index, which is related to pressure and density via the Gladstone–Dale relation. Therefore, the shadowgraph is sensitive to the pressure wave, that is, the shockwave. As a probe light, a CW diode laser (LDM670, Thorlabs) with an output wavelength of 670 nm irradiates the distilled water in the quartz sample cell with a thickness of 10 mm. The probe light was incident on the water sample perpendicular to the shockwave propagation and was imaged by a 4*f*-type lens system onto the image-intensified CCD of the Princeton PI-MAX3 camera. The image capturing system was synchronized to the

timing of the FEL macropulse generation, and gated by a time duration of 10 ns. The time gate was electronically scanned with the delay generator in the PI-MAX3 system. In this system, we observed time evolution of the THz-light-induced phenomena from a nanosecond to a millisecond time scale with a time resolution of 10 ns. Throughout this paper, the background image obtained without the THz light irradiation is subtracted from the original images, and the resultant background-subtracted images are shown in the figures.

Fig. 3(a) (Multimedia view) shows a shadowgraph image of a water sample irradiated by the THz-FEL with an averaged micropulse energy of 20  $\mu\text{J}$ . This energy corresponds to the power density of 3.1  $\text{GW}/\text{cm}^2$  with a pulse width of 1.7 ps and a beam diameter of 0.7 mm. A stripe pattern is clearly seen in the image. Each border line corresponds to a pulse front of shockwaves induced by the THz pulse train. An adjacent shockwave (border line) is one generated by the adjacent THz pulse. Thus, the propagation of the shockwave in water can be obtained from the single captured image. One of the remarkable features is that the THz-light-induced shockwave has a plane wave front. The plane shockwave can be generated from the plane source with loosely focused THz-FEL light, because its beam width of 0.7 mm is much larger than the thickness of the shockwave front,  $\sim 5 \mu\text{m}$ . The plane wave nature causes the long-distance propagation of the shockwave as explained in Fig. 1(b). Fig. 3(b) shows the shockwave amplitude as a function of depth from the air–water interface. The amplitude is obtained by the horizontal sum of the pixel intensities in each row of the shadowgraph image. We emphasize that the shockwave reaches to 3 mm in depth, which is 100 times longer than the skin depth of water for the THz light. This result indicates that the energy of the THz light can be delivered into the water by the shockwave as mechanical energy.

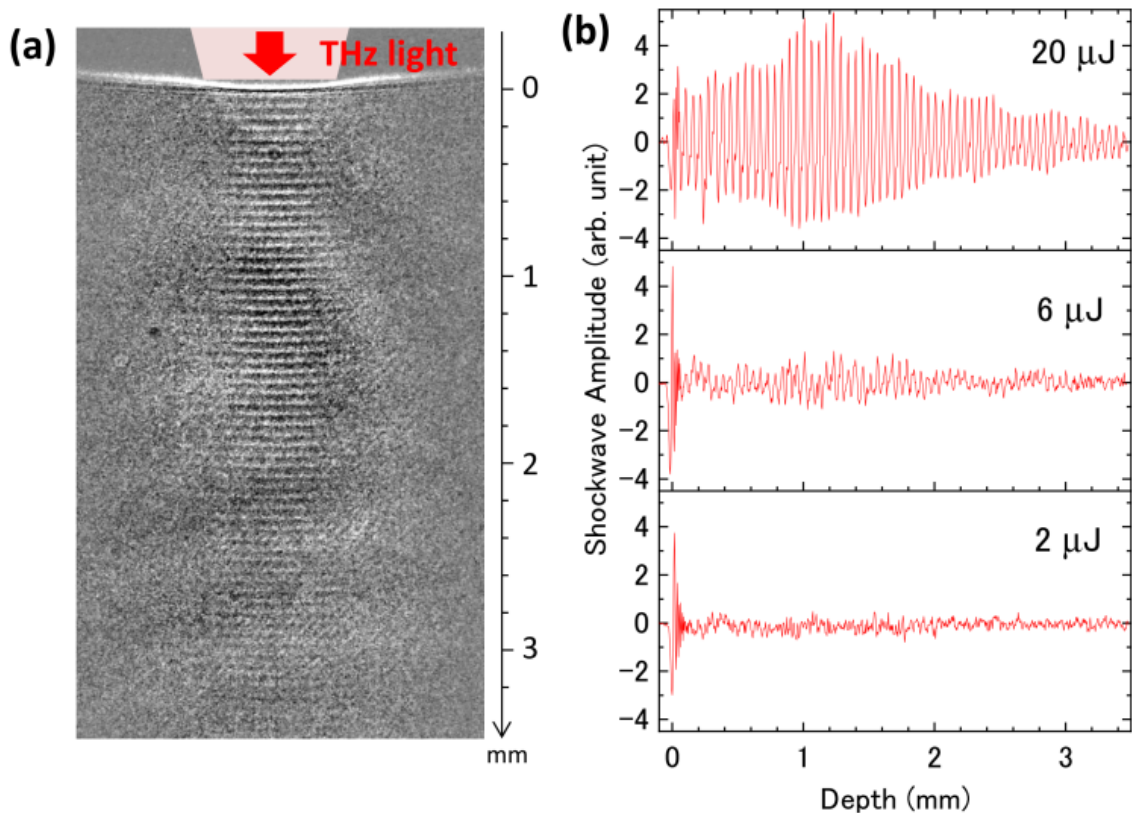


Fig. 3. (Multimedia view) (a) Snapshot image of a train of shockwaves induced by the THz-FEL with a frequency of 4 THz and an averaged micropulse energy of 20  $\mu\text{J}$ . This image was taken with a time gate of 10 ns. The movie consisted of sequential snapshot images are shown in Visualization 1. (b) Shockwave amplitude as a function of depth with the THz micropulse energies of 20, 6, and 2  $\mu\text{J}$ . The amplitude is obtained by the horizontal sum of the pixel intensities in each vertical pixel of the image.

The spacing between shockwave fronts shown in Fig. 3 corresponds to the travelling distance of the shockwave in the time intervals of the THz pulse train, 36.9 ns. Thus, we can obtain the speed of the shockwave in water. To evaluate the speed and the intensity of the shockwaves quantitatively, Fourier transform of the waveform shown in Fig. 3(b) was calculated. Fig. 4(a) shows the shockwave speed as a function of the depth. The speed clearly depends on the depth, being 1528 m/s to 1490 m/s. This means that the shockwave is decelerated during propagation in water. The plausible reason for deceleration is that the local temperature and pressure depends on the depth in water.

The speed of sound is  $c_0 = 1483$  m/s at the room temperature  $20\text{ }^\circ\text{C}$ <sup>20</sup>, and increases as the temperature increases. If the shockwave speed is close to the sound of speed and depends only on the water temperature, the deceleration of the shockwave indicates that the temperature gradually decreases from  $39\text{ }^\circ\text{C}$  (speed of sound = 1528 m/s) at the surface to  $22\text{ }^\circ\text{C}$  (1490 m/s) as the depth increases. The thermal diffusion in liquid water is much slower than the shockwave propagation, and then, the observed temperature gradient would require time for irradiation by multiple THz-FEL macropulses.

The shockwave deceleration is also interpreted as the result of the pressure decreasing due to dispersion of the shockwave during propagation. The weak shock theory in water provides the relation between the shockwave speed  $c_s$  and the local pressure  $p$  as  $c_s = c_0 + \beta p/2\rho c_0$ , where  $\beta$  is the nonlinearity of the water (3.5 at  $20\text{ }^\circ\text{C}$ <sup>21</sup>), and  $\rho$  is the density of water ( $998\text{ kg/m}^3$  at  $20\text{ }^\circ\text{C}$ )<sup>5,22</sup>. If the shockwave speed depends only on the pressure, the deceleration of the shockwave indicates that the local pressure of the shockwave front decreases from  $p = 38$  MPa to 5.9 MPa during propagation.

The THz-light-induced shockwaves with weaker pulse energies are also observed and shown in Fig. 3(b). We clearly see the shockwave with a micropulse energy of  $6\text{ }\mu\text{J}$  ( $0.9\text{ GW/cm}^2$ ), and slightly recognized it with  $2\text{ }\mu\text{J}$  ( $0.3\text{ GW/cm}^2$ ). By calculating the Fourier transform of the waveforms, the speed and amplitude of the shockwaves are obtained and summarized in Fig. 4. The speed has no significant dependence of the THz micropulse energy. On the other hand, the amplitude relating to the local pressure of the shockwave front increases with the pulse energy. The input THz energy dependence suggests that the shockwave deceleration cannot be interpreted with the simple temperature gradient in water and the weak shock theory. We probably have to consider the effect of multi pulses contained in the single macropulse. Because the temperature and the local pressure of the shockwave front are very important parameters for chemical and biological reactions, we have to further investigate the shockwave propagation with thermo and hydrodynamical simulations. Another significant feature in Fig. 4(b) is that there is no obvious threshold of the input THz energy for shockwave generation in contrast to the conventional method triggered by plasma generation with near-IR laser.<sup>5</sup> This is one of evidences that the THz-light- induced shockwave is caused by strong linear absorption of THz light by water.

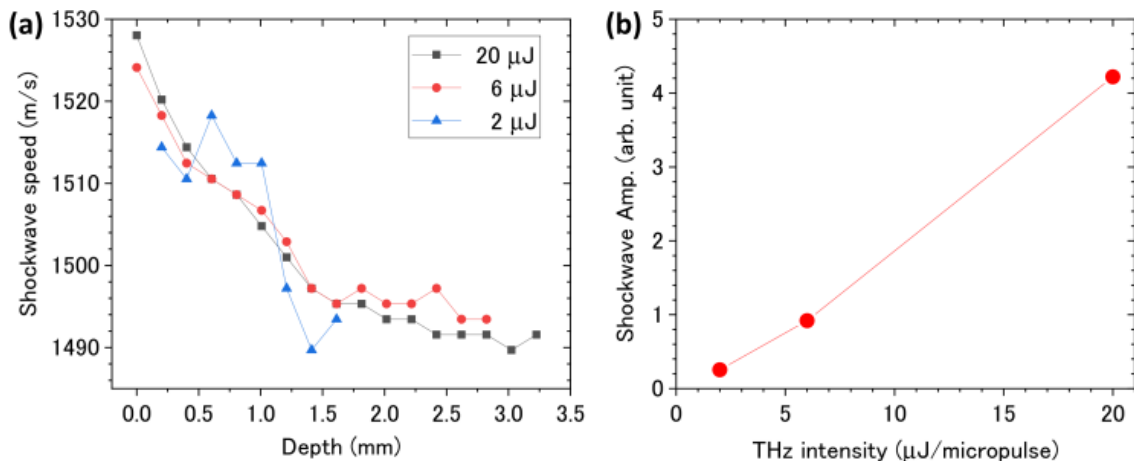


Fig. 4. (a) Shockwave velocity as functions of the depth and THz micropulse energy. The Fourier transform was calculated at each depth with a limited range of  $\pm 0.5$  mm for 20 and  $6\text{ }\mu\text{J}$  and  $\pm 1$  mm for  $2\text{ }\mu\text{J}$ . (b) THz micropulse energy dependence of shockwave amplitude calculated at the depth of 1 mm.

In summary, we demonstrated generation and observation of a THz-light-induced shockwave. The initial process prior to the shockwave generation is linear absorption of the THz light by water as contrasted with plasma generation at the air–water interface by multi-photon absorption of near- or mid-IR light. This provides great advantages for the THz-induced shockwave as compared to the conventional IR-induced methods. First, the linear absorption is a mild and non-destructive process, and therefore, the proposed method can be applied to the biological tissue and fragile instruments. Next, loosely focused THz light can generate the shockwave with a plane wave front because of effective energy transfer from the THz light to the shockwave due to strong linear absorption by water. The propagation of the plane wave is easily controlled with reflective and focusing elements. Third, the THz-light-induced shockwave requires an irradiation energy density,  $0.3 \text{ GW/cm}^2$ , which is smaller than that of  $100 \text{ PW/cm}^2$  required for the IR-induced shockwaves by six orders of magnitude.<sup>5</sup> As a  $2 \mu\text{J}$  pulse at the frequency of 4 THz has recently been produced using a tabletop laser system,<sup>23, 24</sup> the THz-light-induced shockwave system can potentially be moved from the FEL facility to the laser laboratory for the medical and industrial applications.

The large absorption coefficient of the THz light means that the penetration depth in water is considerably shorter than 1 mm. Therefore, the THz light can directly affect the molecules or the biological tissues only within a submillimeter range. In previous studies, THz-light-induced DNA damage to a human skin sample with a thickness of less than 0.1 mm has been examined and discussed.<sup>25-28</sup> THz-light-induced shockwaves will potentially be able to probe and control the chemical reactions and biological structures beyond the penetration depth.

This work was performed under the Cooperative Research Program of “Network Joint Research Center for Materials and Devices.” We are grateful for financial support of QST President’s Strategic Grant (Creative Research). We thank K. Furukawa for his technical support to the THz-FEL operation.

## References

1. E. Abraham, K. Minoshima and H. Matsumoto, *Opt. Commun.* **176**, 441 (2000).
2. C. B. Schaffer, N. Nishimura, E. N. Glezer, A. M. T. Kim and E. Mazur, *Opt. Express* **10**, 196 (2002).
3. A. Vogel and V. Venugopalan, *Chem. Rev.* **103**, 577 (2003).
4. A. Vogel, J. Noack, G. Huttman and G. Paltauf, *Appl. Phys. B* **81**, 1015 (2005).
5. B. D. Strycker, M. M. Springer, A. J. Traverso, A. A. Kolomenskii, G. W. Kattawar and A. V. Sokolov, *Opt. Express* **21**, 23772 (2013).
6. C. E. Bell and B. S. Maccabee, *Appl. Opt.* **13**, 605 (1974).
7. D. C. Emmony, B. M. Geerken and A. Straaijer, *Infrared Phys.* **16**, 87 (1976).
8. G. V. Ostrovskaya and E. N. Shedova, *Izvestiya Akademii Nauk Seriya Fizicheskaya* **61**, 1342 (1997).
9. C. A. Stan, D. Milathianaki, H. Laksmono, R. G. Sierra, T. A. McQueen, M. Messerschmidt, G. J. Williams, J. E. Koglin, T. J. Lane, M. J. Hayes, S. A. H. Guillet, M. N. Liang, A. L. Aquila, P. R. Willmott, J. S. Robinson, K. L. Gumerlock, S. Botha, K. Nass, I. Schlichting, R. L. Shoeman, H. A. Stone and S. Boutet, *Nat. Phys.* **12**, 966 (2016).
10. C. A. Stan, P. R. Willmott, H. A. Stone, J. E. Koglin, M. Liang, A. L. Aquila, J. S. Robinson, K. L. Gumerlock, G. Blaj, R. G. Sierra, S. Boutet, S. A. H. Guillet, R. H. Curtis, S. L. Vetter, H. Loos, J. L. Turner and F.-J. Decker, *J. Phys. Chem. Lett.* **7**, 2055 (2016).
11. H. R. Zelsmann, *J. Mol. Struct.* **350**, 95 (1995).
12. M. Heyden, J. Sun, S. Funkner, G. Mathias, H. Forbert, M. Havenith and D. Marx, *Proc. Natl. Acad. Sci. USA* **107**, 12068 (2010).
13. H. Hoshina, H. Suzuki, C. Otani, M. Nagai, K. Kawase, A. Irizawa and G. Isoyama, *Sci. Rep.* **6**, 27180 (2016).
14. M. Nagai, S. Aono, M. Ashida, K. Kawase, A. Irizawa and G. Isoyama, *New J. Phys.* **19**, 053017 (2017).
15. K. Makino, K. Kato, K. Takano, Y. Saito, J. Tominaga, T. Nakano, G. Isoyama and M. Nakajima, *Sci. Rep.* **8**, 2914 (2018).
16. K. Kawase, R. Kato, A. Irizawa, M. Fujimoto, S. Kashiwagi, S. Yamamoto, F. Kamitsukasa, H. Osumi, M. Yaguchi, A. Tokuchi, S. Suemine and G. Isoyama, *Nucl. Instrum. Methods Phys. Res. Sect. A- Accel. Spectrom. Detect. Assoc. Equip.* **726**, 96-103 (2013).
17. A. Nahata, A. S. Weling and T. F. Heinz, *Appl. Phys. Lett.* **69**, 2321 (1996).
18. Q. Wu and X. C. Zhang, *IEEE J. Sel. Top. Quantum Electron.* **2**, 693 (1996).
19. G. S. Settles, *Schlieren and shadowgraph techniques: Visualizing phenomena in transparent media.* (Springer-Verlag, 2001).
20. M. Greenspan and C. E. Tschiegg, *J. Acoust. Soc. Am.* **31**, 75 (1959).
21. M. F. Hamilton and D. T. Blackstock, *Nonlinear Acoustics.* (Academic Press, 1998).
22. P. H. Rogers, *J. Acoust. Soc. Am.* **62**, 1412 (1977).
23. C. Vicario, A. V. Ovchinnikov, S. I. Ashitkov, M. B. Agranat, V. E. Fortov and C. P. Hauri, *Opt. Lett.* **39**, 6632 (2014).
24. C. Vicario, M. Jazbinsek, A. V. Ovchinnikov, O. V. Chefonov, S. I. Ashitkov, M. B. Agranat and C. P. Hauri, *Opt. Express* **23**, 4573 (2015).
25. G. J. Wilmink and J. E. Grundt, *J. Infrared Millim. Terahertz Waves* **32**, 1074 (2011).
26. L. V. Titova, A. K. Ayesheshim, A. Golubov, R. Rodriguez-Juarez, R. Woycicki, F. A. Hegmann and O. Kovalchuk, *Sci. Rep.* **3**, 2363 (2013).
27. L. V. Titova, A. K. Ayesheshim, A. Golubov, D. Fogen, R. Rodriguez-Juarez, F. A. Hegmann and O. Kovalchuk, *Biomed. Opt. Express* **4**, 559 (2013).
28. A. N. Bogomazova, E. M. Vassina, T. N. Goryachkovskaya, V. M. Popik, A. S. Sokolov, N. A. Kolchanov, M. A. Lagarkova, S. L. Kiselev and S. E. Peltek, *Sci. Rep.* **5**, 7749 (2015).